Photorefractive vibrometer for the detection of high amplitude vibrations on rough surfaces

Philippe Delaye, Sébastien de Rossi, Gérald Roosen

Photorefractive vibrometer for the detection of high amplitude vibrations on rough surfaces

Ph. Delaye, S. de Rossi, G. Roosen

Laboratoire Charles Fabry de l'Institut d'Optique, Unité mixte de recherche 8501 du CNRS, Bat. 503, Centre Scientifique d'Orsay, BP.147, 91403 Orsay Cedex.

Abstract

We present and characterize theoretically and experimentally a photorefractive velocimeter. This device, based on two wave mixing in a rapid photorefractive crystal, measures the instantaneous velocity of a vibrating target. It is particularly adapted to the measurement of high amplitude (as high as some mm) low frequency (until some kHz) vibrations. Instantaneous velocity as high as 25mm.s^{-1} are expected to be measured with common photorefractive semiconductors and CW lasers.

Laser vibrometry is now widely spread in the field of non destructive testing, for the determination of the vibration spectra of objects, as well as for ultrasonic testing of mechanical parts [1]. Vibration sensors are commercially available. Most of these sensors are based on coherent detection schemes (homodyne or heterodyne detections). Although very sensitive, these sensors lose their efficiency when used with scattering surfaces. That often prevents the measurements, unless the object is first polished, what is most of the time not possible. A solution to this problem is brought by the use of adaptive photodetectors for the phase demodulation [2]. These adaptive photodetectors are based either on two wave mixing in a photorefractive crystal or on non steady state photoelectromotive forces in photoconductive materials, with similar performances and specific advantages and drawbacks for both effects. They were successfully used for the detection of acoustic [3] or ultrasonic vibrations [4, 5] but also in many other devices such as free space coherent detection [6], for the dynamic stabilization of holographic recording [7], or for material characterization [8]. Concerning the vibrations measurements, other techniques were developped using time-averaged holography [9], real time double exposure holographic camera [10], or lock-in detections [11], but none of these techniques allows to perform time resolved measurement like adaptive photodetectors. One characteristics of all these devices is that they deal with stationnary holograms and thus consider the case of low amplitude vibrations only, i.e. vibrations of the order of magnitude of the wavelength at maximum, to limit the effect of the erasing of the hologram. The case of high amplitude vibrations has been considered only one time [12], if we except one proposal of a velocimeter [13] that uses a peculiarity of the non steady state photoelectromotive force to generate a DC current proportionnal to the Doppler shift of the two illuminating beams. In both cases the theoretical modeling uses a Fourier series development to determine the response of the device. This approach restricts its use to periodical phase modulation signals and makes the inversion of the problem (i.e. calculating the phase modulation that induces the detected signal) very difficult in case of non periodical vibrations.

In this paper we will describe a photorefractive interferometer derived from the photorefractive ultrasonic sensor, that keeps its main advantage, i.e. the possibility to work with speckled beams, and that extends its measurement ability to high amplitude vibrations (sub millimeter vibrations). A new theoretical description, presented in the first part, will allow to show that in the chosen working regime the device measures the temporal evolution of the instantaneous velocity of the vibrations and thus works as a velocimeter. Then we will present its experimental implementation and first results that clearly demonstrate its differentiating behavior. The experimental results will also be compared to the theoretical predictions.

I. THEORETICAL MODEL

In its principle, the device is based on a two wave mixing experiment in an holographic material. We already used this set-up to develop a photorefractive ultrasonic sensor [5, 14]. The tested point on the object is illuminated by a laser source. The signal wave reflected and scattered by the object is sent on a dynamic holographic material together with a coherent pump beam. These beams write in the holographic material an hologram of the wavefront structure of the signal beam.

This hologram is read by the pump beam what creates in the direction of the transmitted signal beam a local oscillator that has exactly the same wavefront structure than the signal beam, whatever this structure. These two beams will then interfere in a wide field of view homodyne detection scheme, what will transform the phase modulation imprinted on the signal beam (and caused by the vibration of the object) into an intensity modulation. The phase shift between the signal and the local oscillator can be chosen experimentally to be equal to $\pi/2$ (beams in quadrature) in order to optimize the operation of the sensor.

We here consider an object vibrating at low frequency compared to the cut-off frequency of the dynamic holographic material (i.e. the inverse of the response time of the material). In this regime, the hologram follows the vibrating interference pattern with, nevertheless, a delay. This means that the local oscillator will carry some information on the vibration, as it comes from the diffraction of a stationary beam on a mobile hologram.

From a general point of view, we will show that in this low frequency regime the two wave mixing set-up works as a velocimeter. If the phase modulation imprinted on the signal beam is given by a vibration of amplitude $\delta(t)$, we measure a signal proportional to the instantaneous velocity $v(t)$ of the surface. We will also show that the saturation of the signal at high displacement, observed at high frequency and linked to the partial erasure of the hologram, still exists but is less stringent than for the photorefractive ultrasonic sensor. This saturation is linked to the response time of the dynamic holographic material, and at a fixed frequency it is all the more high than this response time is short.

I.1. Beam coupling in the anisotropic diffraction configuration

For presenting the theoretical model, we will consider a photorefractive crystal used in the anisotropic diffraction configuration [5] (Fig.1). In this configuration, two s-polarized signal and pump beams, interfere to create the grating in a photorefractive crystal in the diffusion regime. The pump beam diffracts into a p-polarized local oscillator. Then the two beams (s-polarized signal and p-polarized local oscillator) are sent on a quarter wave plate with axes oriented along the polarization axes. This wave plate induces a $\pi/2$ phase shift between the two beams that are either in or out of phase (depending on the sign of the index grating) at the output of the crystal. The two cross polarized beams are then sent on a 45° polarizing beamsplitter. The beams issued from the beamsplitter are sent on two detectors which signals are subtracted in a differential amplifier. We choose this configuration because it is easy to implement, and it does not require an external applied electric field. It is also differential what can be interesting to eliminate an eventual intensity noise of the laser.

For simplicity of the study, we neglect the absorption of the crystal. We also place ourselves in the undepleted pump approximation, which means that the pump beam amplitude stays constant in the thickness of the crystal (condition usually fulfilled when the pump beam intensity is much higher than the signal beam intensity). In such a case the equation that governs the diffraction of the pump beam E_{ps} on the grating to form the p-polarized signal beam E_{sp}, is :

$$\frac{\partial E_{sp}}{\partial x} = \frac{\gamma}{G}\Delta n(t) E_{ps} \tag{1}$$

where γ is the photorefractive gain in amplitude (real in the diffusion regime we consider), $\Delta n(t)$ is the index grating variation, which temporal evolution is given by first order kinetics, with a real time constant τ, and a steady state that is proportional to the fringe modulation with a proportionality constant G :

$$\frac{\partial \Delta n}{\partial t} + \frac{\Delta n}{\tau} = \frac{G}{\tau}\frac{m(t)}{2} \tag{2}$$

The fringe modulation m, is given by the interference of the s-polarized components of the pump beam E_{ps} and of the signal beam E_{ss} (with the corresponding intensities I_{ps} and I_{ss}) :

$$m(t) = \frac{2\, E_{ss}(t)\, E_{ps}^{*}}{I_{ss}(t) + I_{ps}} \tag{3}$$

If the target vibrates, with an amplitude $\delta(t)$, it induces on the signal beam a phase modulation $\varphi(t) = 4\pi\delta(t)/\lambda$, leading to an amplitude of the s-polarized component of the signal beam (constant on the whole crystal thickness as absorption is neglected) :

$$E_{ss}(t) = E_{ss}\, e^{i\varphi(t)} \tag{4}$$

This phase modulation generates a displacement of the fringe pattern according to a law :

$$m(t) = m_0\, e^{i\varphi(t)} \tag{5}$$

Equation (1) is solved very easily for a crystal of thickness x, using the boundary condition $E_{sp}(x = 0) = 0$:

$$E_{sp}(t) = \frac{\gamma\, x}{G}\Delta n(t) E_{ps} \tag{6}$$

To this equation we have to add the value of the other polarization component of the signal beam that is given by equation (4).

After the crystal the signal beam passes a quarter wave plate, where the p-polarization component is $\pi/2$ phase shifted regarding to the s-polarization. Then both polarization components are sent on a 45° polarizing beamsplitter where they create two beams, having the amplitudes :

$$\begin{cases} E_1(t) = \dfrac{1}{\sqrt{2}}\left[E_{ss}\, e^{i\varphi(t)} + e^{i\pi/2}\dfrac{\gamma\, x}{G}\Delta n(t) E_{ps}\right] \\ E_2(t) = \dfrac{1}{\sqrt{2}}\left[E_{ss}\, e^{i\varphi(t)} - e^{i\pi/2}\dfrac{\gamma\, x}{G}\Delta n(t) E_{ps}\right] \end{cases} \tag{7}$$

Both beams having intensities :

$$\begin{cases} I_1(t) = |E_1(t)|^2 = \dfrac{1}{2}\left[\left|i\dfrac{\gamma\, x}{G}\Delta n(t) E_{ps}\right|^2 + \left|E_{ss}\, e^{i\varphi(t)}\right|^2 + 2\,\mathrm{Re}\left[i\dfrac{\gamma\, x}{G} E_{ps} E_{ss}^{*}\Delta n(t) e^{-i\varphi(t)}\right]\right] \\ I_2(t) = |E_2(t)|^2 = \dfrac{1}{2}\left[\left|i\dfrac{\gamma\, x}{G}\Delta n(t) E_{ps}\right|^2 + \left|E_{ss}\, e^{i\varphi(t)}\right|^2 - 2\,\mathrm{Re}\left[i\dfrac{\gamma\, x}{G} E_{ps} E_{ss}^{*}\Delta n(t) e^{-i\varphi(t)}\right]\right] \end{cases} \tag{8}$$

Both beams are sent on two detectors which signals are subtracted to give :

$$S(t) = 2\,\mathrm{Re}\left[i\frac{\gamma\, x}{G} E_{ps} E_{ss}^{*}\Delta n(t) e^{-i\varphi(t)}\right] \tag{9}$$

That can be rewritten, using relations (5) and (3) :

$$S(t) = \mathrm{Re}\left[i\,\gamma\, x \frac{4 I_{ss} I_{ps}}{\left(I_{ss} + I_{ps}\right)} \frac{\Delta n(t)}{m_0 G} \frac{m^*(t)}{m_0^*} \right] \tag{10}$$

In the general condition of use of a two beam coupling set-up, the intensity of the pump beam is much larger than the one of the signal beam. Thus we have $I_{ss} << I_{ps}$ and S(t) becomes (as γ is real):

$$S(t) = 2\,\gamma\, x\, I_{ss}\, \mathrm{Re}\left[S_C(t)\right] \tag{11}$$

with :

$$S_C(t) = 2\,i \frac{\Delta n(t)}{m_0 G} \frac{m^*(t)}{m_0^*} \tag{12}$$

Using equation (2) together with relation (5), we easily show that $S_c(t)$ is governed by the following differential equation :

$$\frac{\partial S_C}{\partial t} = -S_C\left(i \frac{\partial \varphi}{\partial t} + \frac{1}{\tau} \right) + \frac{i}{\tau} \tag{13}$$

whose solution is :

$$S_C(t) = \frac{i}{\tau} e^{-i\varphi(t)} e^{-\frac{t}{\tau}} \left(\int_0^t e^{i\varphi(t')} e^{\frac{t'}{\tau}} dt' + C \right) \tag{14}$$

Constant C is given by the initial condition. At t=0 $S_C(t)=S_{C0}$, which gives $C = -i\,\tau\, S_{C0}\, e^{i\varphi(0)}$. In the case of a vibration measurement, we usually write the grating until steady-state is reached (i.e. $\Delta n(0) = \Delta n_{st} = \left(G m_0 e^{i\varphi(0)} \right) / 2$) and at time t=0 we apply the vibration with a phase origin $\varphi(0)$. Thus according to relation (12) we have $S_{C0} = i$.

Making the variable change t'=t-u in the integral, we finally arrive at :

$$S_C(t) = \frac{i}{\tau} \int_0^t \cos\left(\varphi(t-u) - \varphi(t)\right) e^{-\frac{u}{\tau}} du - \frac{1}{\tau} \int_0^t \sin\left(\varphi(t-u) - \varphi(t)\right) e^{-\frac{u}{\tau}} du + S_{C0}\, e^{-i(\varphi(t) - \varphi(0))}\, e^{-\frac{t}{\tau}} \tag{15}$$

I.2. Case of a low frequency signal

Until now no supposition has been made concerning the phase modulation characteristics. The above expressions are thus valid whatever the exact nature of the phase modulation (high or low amplitude, or high or low frequency). We now place ourselves in the case we are interested in, i.e. we consider a modulation with a low frequency compared to the inverse of the response time of the dynamic holographic material. This means that the signal varies with a time period much greater than the response time of the material. We have thus $t >> \tau$. As $e^{-\frac{u}{\tau}}$ is non negligible for values of u close to τ only, that means that we can consider that $u << t$ and thus $t-u \approx t$, in the integrals of relation (15). This allows to make a Taylor development of $\varphi(t)$, that gives :

$$\varphi(t-u) - \varphi(t) \approx -u \frac{\partial \varphi}{\partial t} \tag{16}$$

The two integrals of relation (15) can then be explicitly calculated :

$$\int_0^t \sin\left(-u\frac{\partial\varphi}{\partial t}\right) e^{-\frac{u}{\tau}} du = \frac{-\tau^2\frac{\partial\varphi}{\partial t} + \tau e^{-\frac{t}{\tau}}\left[\tau\frac{\partial\varphi}{\partial t}\cos\left(t\frac{\partial\varphi}{\partial t}\right) + \sin\left(t\frac{\partial\varphi}{\partial t}\right)\right]}{\left(1+\tau^2\left(\frac{\partial\varphi}{\partial t}\right)^2\right)} \quad (17a)$$

and :

$$\int_0^t \cos\left(-u\frac{\partial\varphi}{\partial t}\right) e^{-\frac{u}{\tau}} du = \frac{\tau + \tau e^{-\frac{t}{\tau}}\left[-\cos\left(t\frac{\partial\varphi}{\partial t}\right) + \tau\frac{\partial\varphi}{\partial t}\sin\left(t\frac{\partial\varphi}{\partial t}\right)\right]}{\left(1+\tau^2\left(\frac{\partial\varphi}{\partial t}\right)^2\right)} \quad (17b)$$

As we consider that $t>>\tau$, all the terms in $e^{-\frac{t}{\tau}}$ in relations (15) and (17) can be neglected, and $S_C(t)$ becomes :

$$S_C(t) = \frac{i + \tau\frac{\partial\varphi}{\partial t}}{\left(1+\tau^2\left(\frac{\partial\varphi}{\partial t}\right)^2\right)} \quad (18)$$

Coming back to the real signal S(t) we are interested in, we have :

$$S(t) = 2\gamma x I_{ss}\frac{\tau\frac{\partial\varphi}{\partial t}}{\left(1+\tau^2\left(\frac{\partial\varphi}{\partial t}\right)^2\right)} \quad (19)$$

This expression shows that the signal of the two wave mixing interferometer in the low frequency domain depends on the derivative of the phase modulation signal only. If now the amplitude of the phase modulation derivative is small enough, such that $\tau^2\left(\frac{\partial\varphi}{\partial t}\right)^2 << 1$, the expression simplifies and becomes :

$$S(t) = 2\gamma x \tau I_{ss}\frac{\partial\varphi}{\partial t} \quad (20)$$

The signal is directly proportional to the instantaneous velocity of the target. The two wave mixing interferometer thus works as a velocimeter in the low frequency domain.

I.3. Limit of the linear regime

The above point was already established previously but only in the case of a low amplitude phase variation ($\varphi(t)<<\pi/2$) [8, 14]. We see that the previous results apply more largely to large amplitude modulation, as soon as $\tau^2\left(\frac{\partial\varphi}{\partial t}\right)^2 << 1$. For a phase modulation induced by a surface displacement, we have $\varphi(t) = 4\pi\delta(t)/\lambda$ and $\frac{\partial\varphi}{\partial t} = 4\pi v(t)/\lambda$. The condition becomes :

$$\left(\frac{4\pi\tau v(t)}{\lambda}\right)^2 << 1 \quad (21)$$

A good limit for such a condition is :

$$\left(\frac{4\pi\tau v(t)}{\lambda}\right) < \frac{1}{3} \tag{22}$$

which gives :

$$v(t) < v_{lim} = \frac{1}{12\pi}\frac{\lambda}{\tau} \tag{23}$$

The performances of the velocimeter, i.e. the maximum velocity measurable in the linear regime, will be controlled by the response time of the crystal only. The shortest response time will be the best. Considering usual photorefractive crystals used with CW laser, response time of the order of a microsecond should be reachable with the more rapid crystals such as the semiconductors. For a wavelength of 1.06μm and a crystal having a response time of 1μs, the limit velocity is $v_{lim} = 28mm.s^{-1}$.

In the case of a sinusoidal displacement $\delta(t) = \delta_0 \sin(2\pi f t)$, we have $v(t) = 2\pi f \delta_0 \cos(2\pi f t)$, and condition (23) becomes :

$$f\delta_0 < \frac{1}{24\pi^2}\frac{\lambda}{\tau} \tag{24}$$

For the same experimental parameters (λ=1.06μm and τ=1μs) this leads to a maximum measurable displacement of 4.5μm at the frequency of 1kHz, or 4.5mm at a 1Hz frequency.

I.4. Numerical simulation

In order to have an idea of the characteristics of the photorefractive velocimeter, we calculate the response of the system to different incident signals. For this calculation we use expression (11) with $S_C(t)$ given by the solution of the differential equation (13) for a given displacement $\delta(t)$. The parameters of the crystal are a response time τ=1μs, a photorefractive gain in amplitude γ=0.3cm^{-1}, a thickness of 1cm. The calculated values are normalized to the incident signal beam intensity. The first calculation allows to show the derivative behavior of the velocimeter. We see in Fig. 2, the response to a sinusoidal and a sawtooth periodic vibration. For the sinusoidal vibration, the response is phase shifted by a quarter of a period, i.e. the $\pi/2$ phase shift of a cosinusoidal response. Moreover, no deformation of the signal appears, despite the high amplitude of the displacement (1mm). For the sawtooth vibration the response is a square waveform, corresponding to the derivative too.

In Figure 3 we have plotted the response for a fixed amplitude (1mm) as a function of the frequency of the signal. As expected the signal amplitude increases with the frequency until a saturation of the signal, that begins to appear at a frequency of 10Hz, and that becomes clearer at higher frequencies, with a signal that is no more the derivative of the initial signal (curves at 100 and 1000Hz). Then we calculate the response as a function of the amplitude of the vibration at a fixed frequency of 1kHz (Fig.4). The possibility to linearly measure high amplitude vibrations is clearly seen (curves for a displacement amplitude up to 1μm). A saturation at amplitude between 1 and 10μm corresponding to the value given by relation (24) appears, with a deformation of the signal that increases with higher vibration amplitudes due to the apparition of higher harmonics.

We also calculate the RMS value of the signal observed for a sinusoidal vibration of increasing amplitude (from 1nm to 10mm), as a function of the frequency (Fig. 5). At low

amplitude of the vibration (below 100nm), the signal increases linearly as a function of the frequency, until a cut-off frequency of 10^5Hz (corresponding to the 1μs response time). Above this cut-off frequency the signal is constant as the amplitude of the vibration is not sufficient to erase the grating. This regime is the one that corresponds to the photorefractive ultrasonic sensor we previously studied [5, 14]. With higher amplitude of vibrations (above 100nm), the signal increases linearly with the frequency (corresponding to a signal proportional to the velocity) until a maximum value. When the frequency continue to increase the RMS signal decreases as the displacement is sufficient to partially erase the grating (see Fig. 3) and the measured signal is no more sinusoidal. We can note that the maximum RMS signal is independent of the displacement amplitude (except at very low displacement amplitude), it is just the frequency at which this maximum occurs that depends on the displacement.

II. EXPERIMENTAL CHARACTERIZATION

We have experimentally implemented the photorefractive velocimeter, in order to perform a first characterization of its performances, mainly focused here to a verification of its temporal response and its ability to measure high amplitude vibrations.

II.1. Experimental set-up

The set-up is shown in Fig.6. A CW Nd:YAG laser emitting at 1.06μm is split, to form a high power pump beam, and a signal beam that is sent to a piezomirror. The retroreflected beam is mixed with the pump beam into the photorefractive crystal. The photorefractive crystal is a semi-insulating undoped GaAs crystal, used in the anisotropic diffraction geometry, i.e. a grating vector along the (110) direction and the incident beams vertically polarized along (001) axis. The crystal is antireflection coated and has a thickness of 1cm. It is used with a grating spacing of the order of 2μm, the photorefractive gain is 0.13cm^{-1}. After the crystal, the signal beam passes through a quarter wave plate with axes oriented along the direction of the transmitted beam polarization and of the cross polarized diffracted beam. The beam is then sent on a 45° polarizing beamsplitter. The two beams issued from the beamsplitter are sent on two detectors connected to a simple low frequency differential amplifier.

The piezomirror is calibrated and its displacement is measured by an internal sensor, what gives a reference signal. With this piezomirror, displacement amplitudes of 10μm are obtained until frequencies of about 60Hz. These performances are clearly insufficient to characterize the ability of the set-up to measure very high amplitude vibrations, and see its ultimate performances. Nevertheless, this piezomirror is sufficient to realize a first demonstration of the working principle of the photorefractive velocimeter. The characteristics of the crystal (especially a relatively long response time) are chosen in order to see the different operating regimes of the velocimeter (linear regime and saturation regime), with this piezomirror.

II.2. Experimental results

The first experiment (Fig. 7) allows to illustrate the derivative behavior of the photorefractive velocimeter. As expected, the sawtooth signal is transformed into to a square shape periodic signal, whereas the sinusoidal signal is $\pi/2$ phase shifted compared to the initial displacement. We also see that there is no deformation of the sinusoidal response despite the high amplitude of the displacement (2μm), showing the ability for the velocimeter to measure high amplitude signals without the wrapping that is seen in an homodyne detection. For the frequency response of the velocimeter, we see (Fig. 8) that the signal increases with the frequency and saturates for high frequencies (6Hz curve), before being distorted (62Hz curve). The theoretical curves calculated with relations (11) and (13), correspond to the experimental ones when the response time of the crystal (i.e. the only adjustable parameter) that governs the shape of the curves is about 200μs. This gives an idea of the response time of the crystal in this specific experimental arrangement. The saturation begins to occur around 0.6Hz for the 11.4μm displacement amplitude used. This corresponds to what can be found using equation (24).

For the response as a function of the amplitude, there is also a good accordance between calculated and experimental curves (Fig. 9). For the fixed frequency of 62Hz used, the saturation occurs around 144nm which still corresponds to what is given by relation (24). Here again the signal is distorted at higher displacement.

III. CONCLUSION

We present a first characterization of a new holographic vibration sensor, the photorefractive velocimeter. This sensor measures linearly the instantaneous velocity of high amplitude (several μm), low frequency (0 - 1kHz) vibrations on scattering surfaces. We develop a simple theoretical model that perfectly explains the behavior of the velocimeter. The performances of this velocimeter are controlled by the response time of the photorefractive crystal. Using rapid photorefractive crystals like GaAs or CdTe will allow to measure vibration velocities as high as 25mm.s^{-1}. The proof of principle of this photorefractive velocimeter is successfully demonstrated. We will now optimize its performances, to be able to measure such high vibration velocities, with a compact and low cost system.

The device is essentially made for the detection of longitudinal displacement (i.e. along the line of sight), but signals given by the transversal displacement of the speckle pattern will also superimpose to the response. A lot of care in further studies will have to be taken to reduce the sensitivity of the device to this transversal displacement, playing for example with the size of the speckle grains received the sensor.

REFERENCES

[1] J.P. Monchalin, IEEE transactions on ultrasonics, ferroelectrics and frequency control, **UFFC-33**, 485 (1986).

[2] M.P. Petrov, S.I. Stepanov, A.V. Khomenko, “Photorefractive crystals in coherent optical systems”, Springer-Verlag Berlin Heidelberg (1991).

[3] T.J. Hall, M.A. Fiddy, M.S. Ner, Opt. Lett. **5**, 485 (1980)

[4] Yu.O. Barmenkov, V.V. Zosimov, N.M. Kozhevnikov, L.M. Lyamshev and S.A. Sergushchenko, “Investigation of small ultrasonic vibrations by optical dynamic holography techniques”, Sov. Phys. Dokl. **31** (1986) 817.

[5] Ph. Delaye, A. Blouin, D. Drolet, L.A. de Montmorillon, G. Roosen, J.P. Monchalin. J. Opt. Soc. Am. **B 14**, 1723 (1997).

[6] F.M. Davidson, C.T. Field, "Coherent homodyne optical communication receivers with photorefractive optical beam combiners", J. Lightwav. Tech. **12**, 1207 (1994).

[7] A. Kamshilin, J. Frejlich, L.H.D. Cescato, Appl. Opt. **25**, 2375 (1986)

[8] B. Sugg, K.V. Shcherbin, J. Frejlich. Appl. Phys. Lett. **66**, 3257 (1995).

[9] J.P. Huignard, J.P. Herriau, T. Valentin. Appl. Opt. **16**, 2796 (1977)

[10] L. Labrunie, G. Pauliat, J.C. Launay, S. Leidenbach, G. Roosen. Opt. Commun. **140**, 119 (1997).

[11] T.C. Hale, K.L. Telschow, V.A. Deason, Appl. Opt. **36**, 8248 (1997)

[12] I.A. Sokolov, S.I. Stepanov, Appl. Opt. **32**, 1958 (1993)

[13] C.C. Wang, F. Davidson, S. Trivedi, Appl. Opt. **34**, 6496 (1995)

[14] Ph. Delaye, L.A. de Montmorillon, G. Roosen. Opt. Commun. **118**, 1549 (1995).

Figure captions

Figure 1 : Scheme of a photorefractive beam combiner based on the anisotropic diffraction configuration. PBS is a polarizing beam splitter, PC is the photorefractive crystal, λ/2 and λ/4 are half and quarter wave plates respectively.

Figure 2 : Numerical simulation of the velocimeter response, for a sinusoidal (plain lines) and a sawtooth displacement (dashed lines) of 1mm amplitude at 1Hz. Bold line represents the calculated signal and thin lines deals with the initial displacement.

Figure 3 : Numerical simulation of the velocimeter response, for a sinusoidal displacement of 1mm amplitude at different frequencies (the abscissa are normalized to the frequency for comparison of the different curves).

Figure 4 : Numerical simulation of the velocimeter response, for a sinusoidal displacement at 1kHz. The curves at the lowest amplitudes (0.01μm to 1μm) are compensated for their amplitude. They superpose exactly showing the linearity of the response of the velocimeter.

Figure 5 : Frequency response of the photorefractive velocimeter, for different amplitude of the sinusoidal displacement between 1nm and 10mm. The presented signal is the RMS value of the calculated temporal response of the velocimeter.

Figure 6 : Scheme of the experimental set-up used in the study.

Figure 7 : Experimental response of the photorefractive velocimeter to a sinusoidal (black curves) and a sawtooth (grey curves) phase modulation of 0.6Hz frequency. The dashed lines represent the displacement of the piezomirror that creates the phase modulation.

Figure 8 : Experimental response (A) of the photorefractive velocimeter to a sinusoidal phase modulation of fixed amplitude (11.4μm, except for the 62Hz signal corresponding to a 9.9μm displacement amplitude) having an increasing frequency. In (B) are shown the calculated responses of the photorefractive velocimeter.

Figure 9 : Experimental response (A) of the photorefractive velocimeter to a sinusoidal phase modulation of fixed frequency (60Hz) and of increasing amplitude. In (B) are shown the calculated responses of the photorefractive velocimeter.

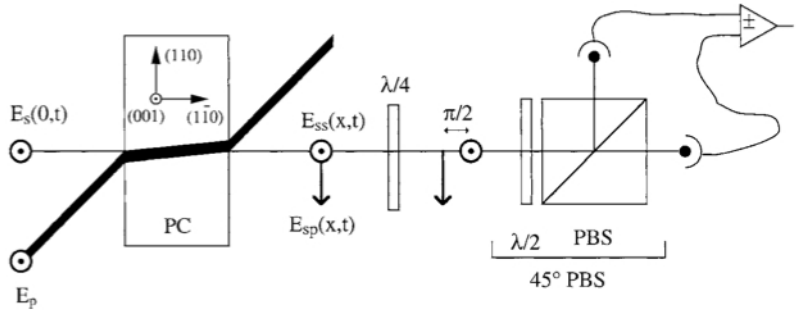

Figure 1

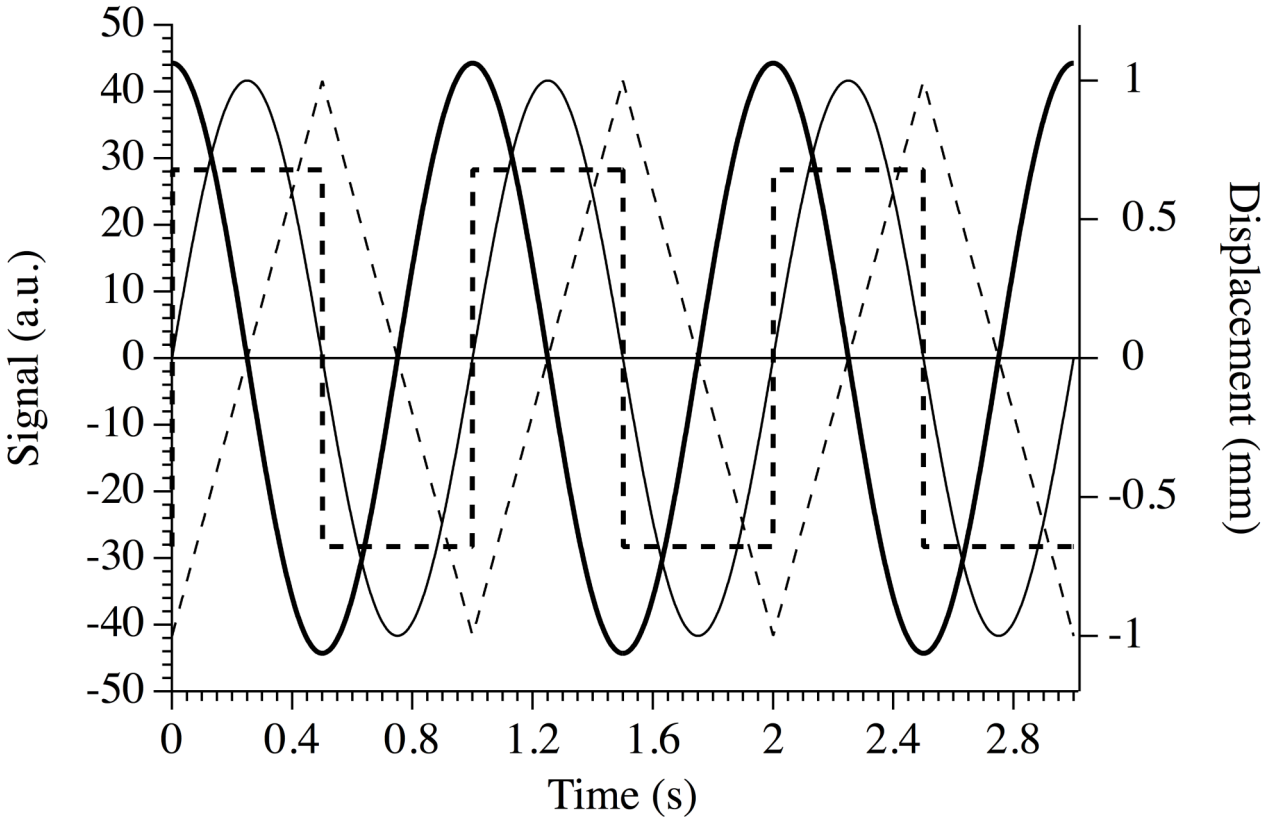

Figure 2 Delaye et al.

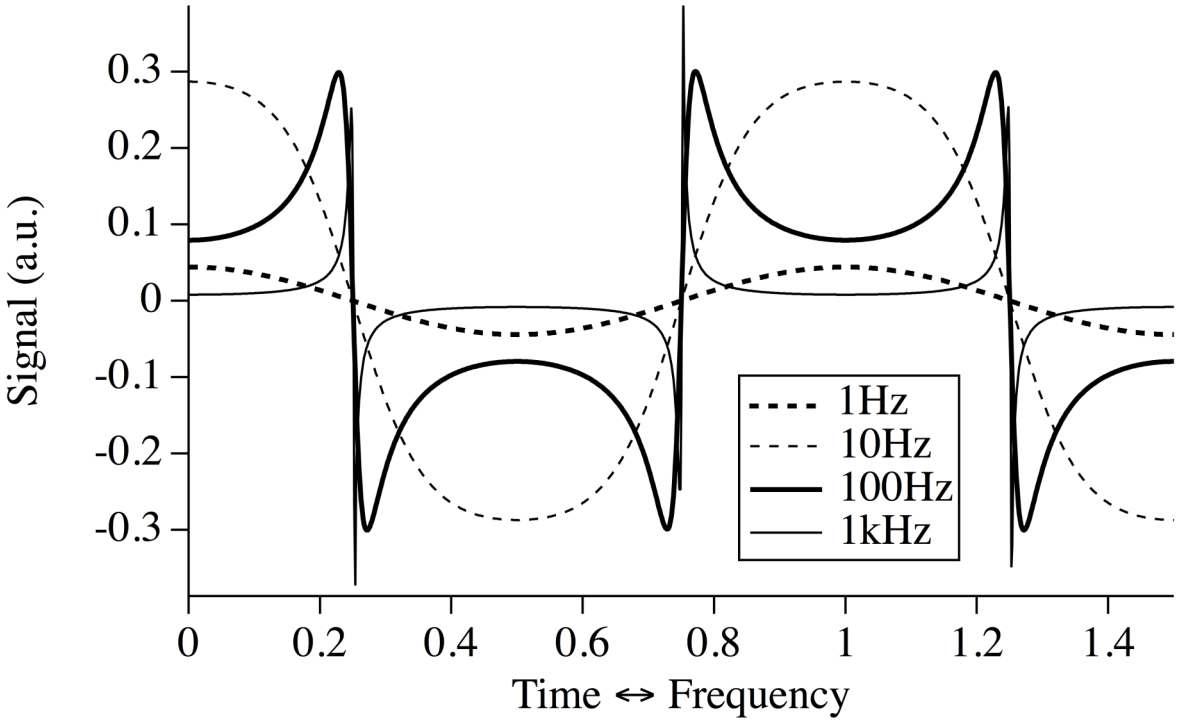

Figure 3 Delaye et al.

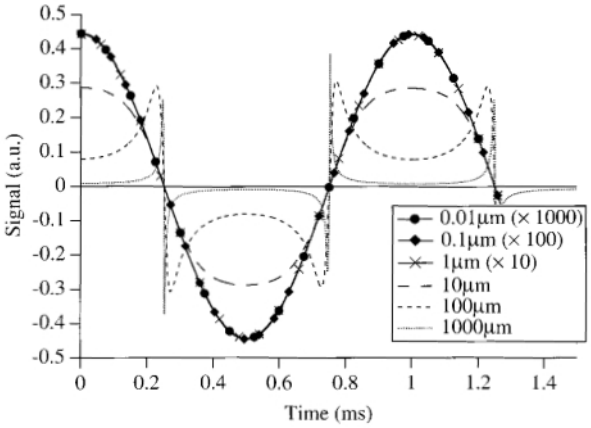

Figure 4

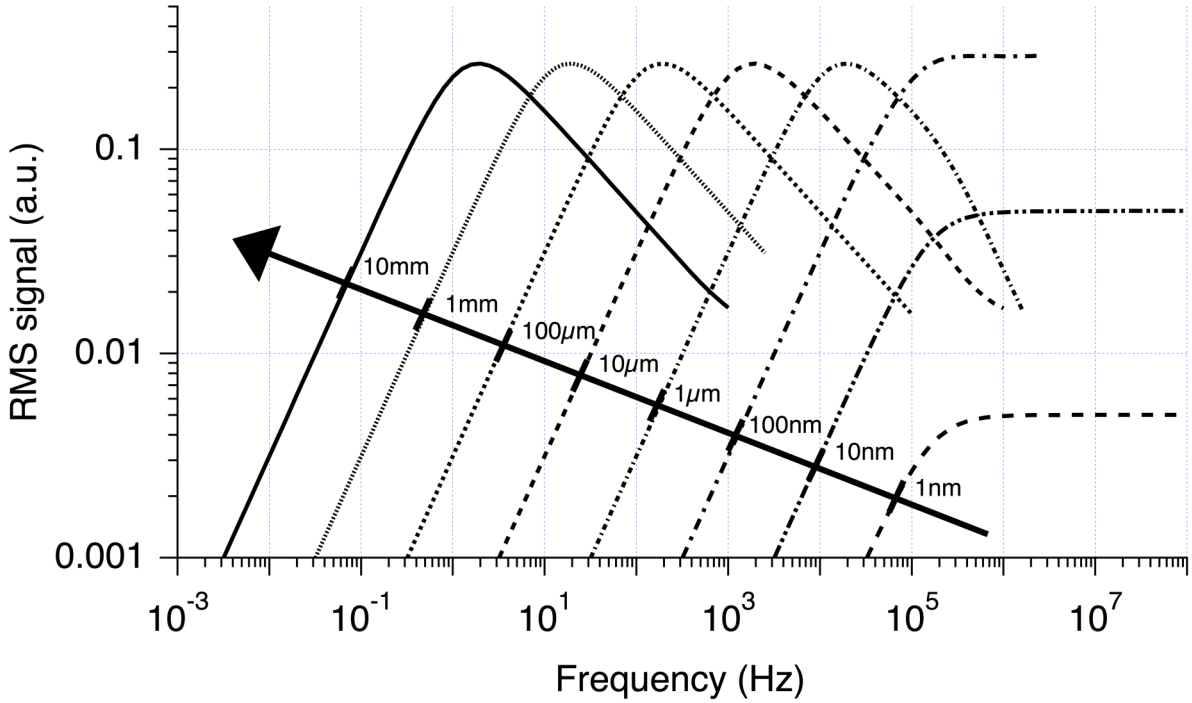

Figure 5 Delaye et al.

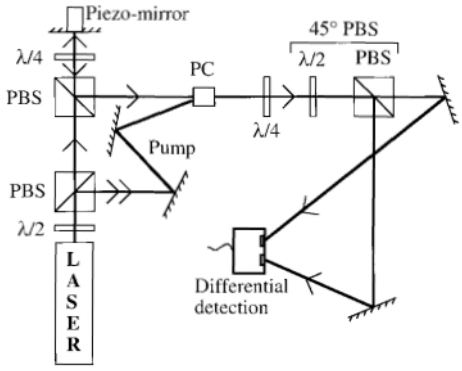
Piezo-mirror
45° PBS
λ/4
λ/2
PBS
PC
PBS
λ/4
Pump
PBS
λ/2
LASER
Differential
detection

Figure 6

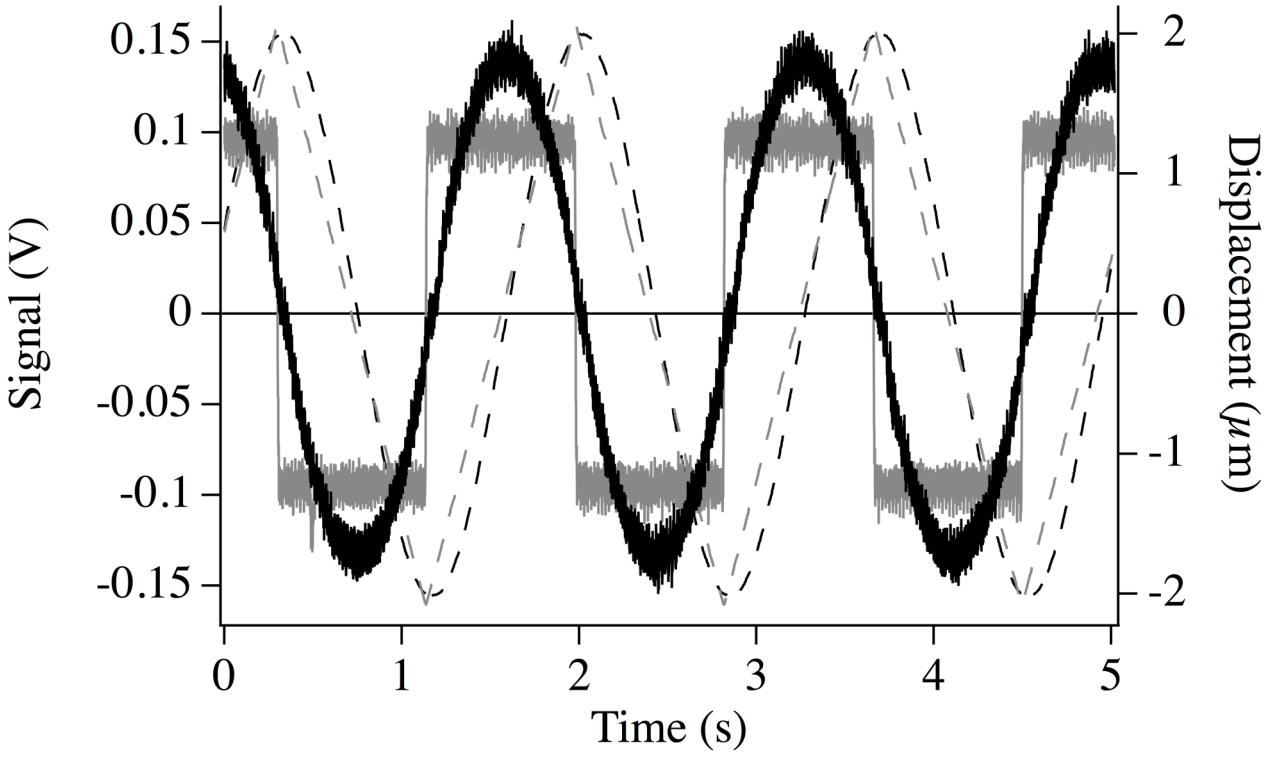

Figure 7 Delaye et al.

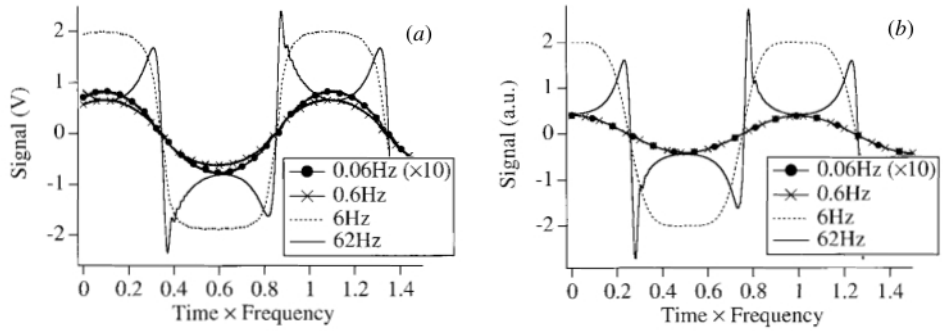

Figure 8

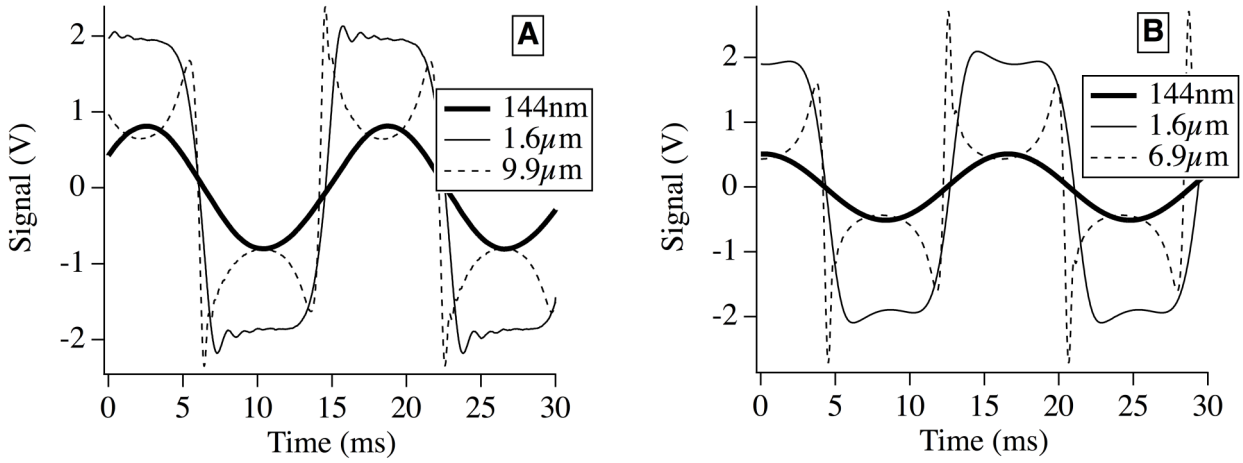

Figure 9 Delaye et al.